Proc. Natl. Acad. Sci. USA
Vol. 95, pp. 4696–4701, April 1998
Neurobiology

An isoform of the rod photoreceptor cyclic nucleotide-gated channel β subunit expressed in olfactory neurons

ANDREA SAUTTER, XIANGANG ZONG, FRANZ HOFMANN, AND MARTIN BIEL*

Institut für Pharmakologie und Toxikologie der Technischen Universität München, Biedersteiner Strasse 29, 80802 Munich, Germany

Edited by Joseph A. Beavo, University of Washington School of Medicine, Seattle, WA, and approved February 4, 1998 (received for review November 11, 1997)

ABSTRACT **Sensory transduction in olfactory neurons involves the activation of a cyclic nucleotide-gated (CNG) channel by cAMP. Previous studies identified a CNG channel α subunit (CNG2) and a β subunit (CNG5), which when heterologously expressed form a channel with properties similar but not identical to those of native olfactory neurons. We have cloned a new type of CNG channel β subunit (CNG4.3) from rat olfactory epithelium. CNG4.3 derives from the same gene as the rod photoreceptor β subunit (CNG4.1) but lacks the long, glutamic acid-rich domain found in the N terminus of CNG4.1. Northern blot and *in situ* hybridization revealed that CNG4.3 is expressed specifically in olfactory neurons. Expression of CNG4.3 in human embryonic kidney 293 cells did not lead to detectable currents. Coexpression of CNG4.3 with CNG2 induced a current with significantly increased sensitivity for cAMP whereas cGMP affinity was not altered. Additionally, CNG4.3 weakened the outward rectification of the current in the presence of extracellular Ca^{2+}, decreased the relative permeability for Ca^{2+}, and enhanced the sensitivity for L-*cis* diltiazem. Upon coexpression of CNG2, CNG4.3, and CNG5, a conductance with a cAMP sensitivity greater than that of either the CNG2/CNG4.3 or the CNG2/CNG5 channel and near that of native olfactory channel was observed. Our data suggest that CNG4.3 forms a subunit of the native olfactory CNG channel. The expression of various CNG4 isoforms in retina and olfactory epithelium indicates that the CNG4 subunit may be necessary for normal function of both photoreceptor and olfactory CNG channels.**

Olfactory sensory neurons of vertebrates respond to odours by rapid cAMP formation followed by the opening of a Ca^{2+} permeable-cyclic nucleotide-gated (CNG) channel (1, 2). The resulting Ca^{2+} entry into the cell then opens a Ca^{2+}-activated Cl^- channel, which carries 70–80% of the depolarizing current of olfactory neurons (3). The olfactory CNG channel is supposed to have a heterotetrameric structure containing at least two different types of subunits, the α subunit (CNG2) and the β subunit (CNG5) (ref. 4; for nomenclature of CNG channel subunits, see ref. 5). The CNG2 subunit (original designation OCNC1, ref. 6) reveals a high degree of sequence identity to the α subunits expressed in rod (CNG1; ref. 7) and cone (CNG3, refs. 8 and 9) photoreceptors and like these subunits, induces the formation of a functional, homomeric CNG channel when heterologously expressed. By contrast, the CNG5 subunit (original designation OCNC2; refs. 10 and 11), like the β subunit of rod photoreceptors (CNG4, refs. 12–15), cannot form functional, cyclic nucleotide-activated channels on its own. However, CNG5 assembles with CNG2 to create a channel with modified properties. A major effect of CNG5 observed upon coexpression with CNG2 is the increase of the channel affinity for cAMP (10, 11). This increase is physiologically very important because cAMP is the natural second messenger of olfaction (1, 2, 16). However, the heteromeric CNG2/CNG5 channel still reveals about a threefold lower affinity to cAMP than the native channel (10, 11, 17). This discrepancy might be explained by the lack of posttranslational modifications or interactions with cellular factors in the heterologous expression system but also may point to the presence of a not yet identified CNG channel subunit. Recently, it has been shown that sensory neurons of the vomeronasal organ lack the CNG2 subunit but express a homomeric CNG5 channel that is opened by NO (18, 19). This finding suggests that CNG5 also may form a NO-gated channel in olfactory neurons of the nasal cavity and raises the question whether CNG channels exist in these neurons that are composed of CNG2 and a β subunit different from CNG5.

We therefore have reexamined expression of CNG channel RNAs in rat olfactory epithelium. We found that olfactory neurons contain in addition to the known olfactory subunits CNG2 and CNG5 a specific isoform of the rod photoreceptor β subunit (CNG4.3). We demonstrate that CNG4.3 assembles with CNG2 to form a functional heteromeric CNG channel that displays properties of the native olfactory CNG channel.

MATERIALS AND METHODS

Cloning Strategy. An oligo(dT)-primed cDNA library was constructed in the pcDNA2 vector (Invitrogen) from 10 μg of poly(A)$^+$ mRNA of rat olfactory epithelium and screened with an 894-base pair (bp) cDNA fragment corresponding to amino acids M_{725}–H_{1022} of the CNG channel β subunit from rat pineal gland, CNG4.1 (20), which also is expressed in rod photoreceptors (A.S., unpublished results). Thirty-four independent clones were obtained. The sequence of rat CNG4.3 shown in Fig. 1 derives from clone pCG62, which contains a 5.0-kilobase (kb) insert. The 5′-untranslated sequence, the coding region, and part of the 3′-untranslated region of pCG62 have been sequenced on both strands. The primary structure of rat CNG4.3 was verified by partial sequencing of several independent clones.

Analysis of Intron/Exon Structure of the Rat CNG4 Gene. Expand long template PCR (Boehringer Mannheim) was performed with genomic DNA of rat liver and eight primer pairs specific for the rat CNG4 sequence covering the distance between exons β1 and β5 (nomenclature of exons and introns corresponding to ref. 14). Primer sequences are available on request. The PCR profile was as follows: denaturation at 94°C for 2 min, 10 cycles with 93°C for 0.5 min, 57°C for 1 min, and

The publication costs of this article were defrayed in part by page charge payment. This article must therefore be hereby marked "*advertisement*" in accordance with 18 U.S.C. §1734 solely to indicate this fact.

This paper was submitted directly (Track II) to the *Proceedings* office.
Abbreviations: CNG, cyclic nucleotide-gated; HEK, human embryonic kidney; GARP, glutamic acid-rich protein.
Data deposition: The sequence reported in this paper has been deposited in the GenBank database (accession no. AJ000515).
*To whom reprint requests should be addressed. e-mail: biel@ipt.med.tu-muenchen.de.

FIG. 1. Primary structure of the rat CNG4.3 subunit. (*Upper*) Scheme of the coding region of CNG4.3. The putative transmembrane segments (1–6), the pore (P), and the cyclic nucleotide-binding domain (CNBD) are indicated. The unique N terminus of CNG4.3 is represented as an open box. (*Lower*) Amino acid sequence of CNG4.3. The unique N terminus encoded by exon β4a is boxed. The transmembrane segments, the pore region, and CNBD are underlined.

68°C for 4 min followed by an additional 30 cycles with a time increment of 10 sec/cycle in the extension time. The obtained PCR fragments were analyzed by Southern hybridization and sequenced partially.

***In Situ* Hybridization.** ^{35}S-labeled riboprobes were synthesized *in vitro* in the presence of [^{35}S]UTP using either T3 or T7 RNA polymerase (Stratagene) for sense or antisense direction, respectively. DNA fragments representing the different probes were subcloned into a modified pUC19 vector (pAL1, ref. 21). The CNG4 common probe template was a 199-bp cDNA fragment corresponding to amino acids V_{528}–R_{594} of CNG4.3. The olfactory-specific template (293 bp) was derived by PCR from the 5′-untranslated region of CNG4.3 (forward primer: 5′-TCCATGCTGTGCCAATCACA; reverse primer 5′-CTGGTCCACATCAGCCTGCA). *In situ* hybridization was performed as described (21). Labeled slides were exposed for 6 days or 8 wk to Kodak Bio Max film and Kodak NTB-2 film emulsion, respectively. After development, slides were counterstained with hematoxylene/eosine and coverslipped.

Northern Analysis. Total RNA was isolated from rat retina and olfactory epithelium, size-fractionated on a 1.0% agarose gel, transferred to Hybond-N membranes (Amersham) and cross-linked by UV light. Three ^{32}P-labeled probes were used: an 894-bp fragment (probe a) derived from the CNG4 transmembrane region, which also was used for screening of the cDNA library, a 293-bp fragment (probe b) derived from the 5′ end of CNG4.3, which also was used as *in situ* hybridization probe, and an 830-bp fragment corresponding to the peptide M_1–A_{277} of rat CNG5 (10, 11). Hybridization was at high stringency as described (22). After development, autoradiographs were scanned digitally and arranged by using CORELDRAW software, Ottawa, Canada.

Expression in Human Embryonic Kidney (HEK) 293 Cells. Recombinant plasmids CG4.3/pcDNA3 and CG5/pcDNA3 were used for transient expression of CNG4.3 and CNG5 in HEK 293 cells (9). CG4.3/pcDNA3 was constructed by ligating the PCR-generated 237-bp *Hin*dIII-Acc65I fragment containing a consensus sequence for initiation of translation (5′-gccgccaccATG-3′) and the 2.5-kb Acc65I-*Xho*I fragment of pCG62 into the *Hin*dIII-*Xho*I site of the pcDNA3 vector (Invitrogen). CG5/pcDNA3 was constructed using a similar approach by subcloning the complete coding region of CNG5 (11) into the *Hin*dIII-*Xba*I site of the pcDNA3 vector. For expression of the CNG2 subunit, the plasmid pCG357/CMV (9) containing the cDNA of the rabbit olfactory CNG2 subunit that reveals 95% sequence identity with rat CNG2 was used. Transient expression was performed as described (9). For coexpression experiments, equimolar amounts of CNG channel subunits were used unless otherwise noted.

Electrophysiology. Current recording from excised inside-out patches was as described (9). The divalent cation-free solution contained 140 mM sodium chloride, 5.0 mM potassium chloride, 10 mM Hepes, and 1.0 mM EGTA (pH 7.4). Measurements with Ca^{2+}-free solutions were performed under symmetrical ionic conditions. The Ca^{2+}-containing solution was comprised of 140 mM sodium chloride, 5.0 mM potassium chloride, 10 mM calcium chloride, and 10 mM Hepes (pH 7.4). Cyclic nucleotides were applied by a multibarrelled perfusion pipette that allowed solution changes within 100 ms. The membrane potential was held at 0 mV and stepped to ±105 mV. Capacitative transients and leak currents were subtracted using currents recorded under the superfusion with solution without an agonist. Data were digitized at 10 kHz, filtered at 2 kHz, and analyzed with AutesP (npi electronic, Tamm, Germany). Dose-response curves for cGMP and cAMP were generated by measuring the current response at +60 mV and were fitted with Hill equation: $I/I_{max} = [C]^{\nu}/([C]^{\nu} + K_a{}^{\nu})$, where $[C]$ is the cyclic nucleotide concentration, K_a is the activation constant, and ν is the Hill coefficient. The relative Ca^{2+}-permeability ($P_{Ca^{2+}}/P_{Na^+}$) was calculated with the modified Goldman–Hodgkin–Katz equation (23) by measuring the reversal potential. All of the experiments were done at room temperature (20°C–22°C). All values are given as mean ± SEM.

RESULTS

In an attempt to identify new CNG channel subunits present in the olfactory system, we screened a cDNA library constructed from rat olfactory epithelium with a probe derived from the transmembrane region of the CNG4.1 subunit (20), which is expressed in rat pineal gland and rod photoreceptors. Thirty-four positive clones were obtained. Sequence and restriction analysis revealed that all of the clones were derived from the same primary transcript. The ORF was encoded for a protein of 858 aa with a molecular mass of 96 kDa (Fig. 1). Sequence comparison with known CNG channel sequences revealed that the protein was an isoform of the rat CNG4 gene. The new subunit was designated as CNG4.3. CNG4.3 is identical with photoreceptor and pineal gland CNG4 isoforms (CNG4.1 and CNG4.2, ref. 20) in the transmembrane core and the C terminus but contains a unique sequence of 74 aa at the N terminus. In addition, it lacks the long, glutamic acid-rich domain, which is present in photoreceptor CNG4 subunits (13–15, 20). In photoreceptors and pineal gland, the glutamic acid-rich domain also is expressed as a distinct soluble protein, the glutamic acid-rich protein (GARP; refs. 13, 15, 20, 24, and 25). Screening of the olfactory library with a GARP-specific probe did not result in the identification of positive clones indicating that GARP-specific mRNA, whether at all, is present only at a very low amount in olfactory epithelium.

We partially have characterized the intron/exon organization of the genomic region of the rat CNG4 gene that is processed differentially in rod photoreceptors and olfactory neurons (Fig. 2). The unique N terminus of CNG4.3 is encoded by the specific exon β4a that is localized between exons β4 and β5 (nomenclature of exons according to ref. 14). Exon β4a also

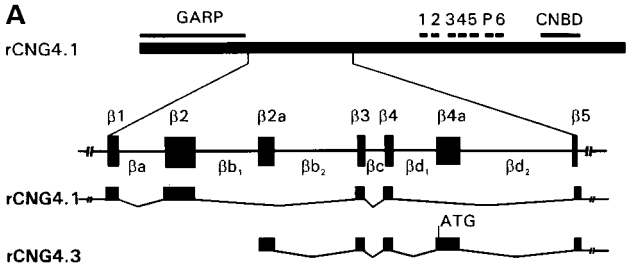

B

exon	exon length	donor	acceptor	intron length	intron
β1	160	gtgggaaaag..		1800	βa
β2	369			2500	βb_1
β2a*	(175)	gtaggtggcc..	..ttcgtcacag	3300	βb_2
β3	88			750	βc
β4	127	gtaggagtga..	..ccgattacag	1700	βd_1
β4a	268	gtatgtgat..	..ctctccccag	4800	βd_2
β5	157				

FIG. 2. Structure of the CNG4 gene locus that is differentially transcribed in rat olfactory neurons and retina. (*A, Upper*) Primary structure of the long CNG4 isoform expressed in rat retina and pineal gland (CNG4.1). The location of the GARP-domain, the transmembrane segments and the CNBD is indicated. (*A, Bottom*) Schematic representation of introns and exons representing the region between GARP- and the transmembrane domain. The transcripts that are expressed in retina (CNG4.1) and olfactory neurons (CNG4.3) arise from differential processing of the indicated genomic sequence and are shown below the exon–intron structure. Exons are represented by filled rectangles (β1–β5), the intervening introns are shown by thin lines (βa–βd_2). The transcript of CNG4.3 starts with exon β2a; the initiating methionine is localized on exon β4a. In CNG4.1 exons, β2a and β4a are skipped. β3 and β4 are coding exons in CNG4.1 and noncoding exons in CNG4.3. The localization of exons upstream of β1 and downstream of β5 has not been determined. (*B*) Intron/exon organization of the rat CNG4 gene. The intron sizes were estimated by PCR. All determined donor and acceptor sequences conformed to the GT–AG rule (30). The exact starting point of CNG4.3 transcription has not been determined. Therefore, the 5′-end of the exon β2a is not known. A lower limit for the size of β2a (175 bp) was deduced from the sequence of the longest cDNA clone isolated (pCG62).

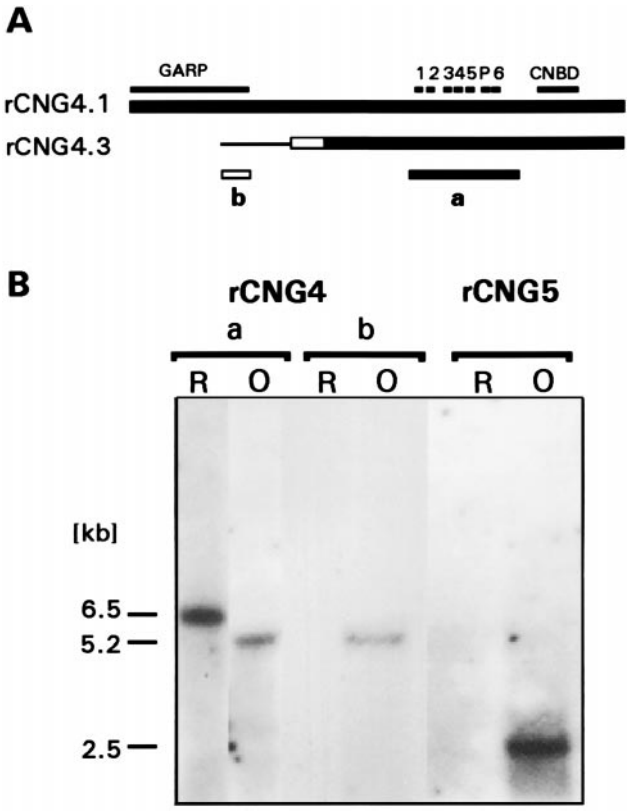

FIG. 3. Northern analysis of CNG subunit transcripts expressed in rat retina and olfactory epithelium. (*A*) Scheme showing the location of probes a and b used for Northern analysis. The protein coding region of CNG4.1 and CNG4.3 are shown as boxes. The GARP-domain, the transmembrane segments, the pore, and the CNBD are indicated. The unique amino terminus and the 5′-untranslated sequence of CNG4.3 are shown as a white box and a thin line, respectively. The location of probes a and b are indicated below the CNG4.3 protein. (*B*) Northern analysis of CNG4 and CNG5 expression. Ten micrograms of total RNA isolated from rat retina (R) and olfactory epithelium (O) were analyzed with CNG4-specific probes a and b and with a CNG5-specific probe (see *Materials and Methods*). Autoradiographic exposure was for 6 days at −70°C for all three probes.

encodes part of the 5′-untranslated region. The residual 5′-untranslated region of CNG4.3 is encoded by three exons, β2a, β3, and β4. Exon β2a resides within exons β2 and β3 and is present only in the CNG4.3 transcript. Interestingly, exons β3 and β4 are coding exons in photoreceptor CNG4 transcripts whereas they are noncoding in CNG4.3.

We performed Northern blot analysis to investigate the expression of CNG channel β subunits in rat retina and olfactory epithelium (Fig. 3). A probe derived from the transmembrane region of CNG4 (probe a) recognized transcripts of 6.5 kb and 5.2 kb in retina and olfactory epithelium, respectively. The size of the olfactory transcript is in good agreement with the length of the cloned CNG4.3 sequence. A transcript of the same size also was identified in olfactory mRNA with probe b derived from the olfactory-specific exon β2a, and with a probe derived from the first coding exon β4a (not shown) verifying the integrity of the cloned CNG4.3 sequence. By contrast, probe b failed to detect a transcript in retina. Similarly, the 2.5-kb transcript of the CNG5 subunit could be identified in olfactory epithelium but was absent from retina (Fig. 3*B*).

In situ hybridization experiments further demonstrated the expression of CNG4.3 in the olfactory epithelium. Fig. 4*A-C* show coronal sections through the nasal cavity of an adult rat that were hybridized to a ^{35}S-labeled antisense RNA probe directed against the 5′-region of the CNG4.3 transcript. Labeling was detected throughout the entire extent of the olfactory epithelium (Fig. 4*A*). The same expression pattern was observed with a probe specific for the CNG4 transmembrane region and with probes specific for the CNG2 and the CNG5 subunit (not shown). Examination of the epithelial sections at higher magnification (Fig. 4 *B* and *C*) showed that only the olfactory neuronal layer is labeled. With a sense probe, no hybridization was observed (Fig. 4*D*). Transcripts of the rod (CNG1) and cone (CNG3) photoreceptor α subunits were not detectable in olfactory epithelium by *in situ* hybridization (not shown). In summary, the Northern blot and *in situ* hybridizations indicated that CNG4.3 is: (*i*) expressed specifically in olfactory sensory neurons and (*ii*) may be colocalized with the CNG5 subunit and the CNG2 subunit.

To determine whether CNG4.3 alone could form a functional CNG channel, we transiently transfected HEK293 cells with a CNG4.3 expression vector. As has been reported for other CNG4 isoforms (12, 13, 22), CNG4.3 failed to induce the formation of a cyclic nucleotide-gated conductance. Channel activity also was undetectable upon coexpression of CNG4.3 and CNG5 (not shown). To evaluate whether CNG4.3 could alter properties of the CNG2 channel, we transfected HEK293 cells with the CNG2 expression vector alone or combined with the CNG2 and CNG4.3 plasmids in equimolar ratio. CNG4.3 had profound influence on the affinity for cAMP. At +60, mV cells expressing CNG2 alone displayed a cyclic nucleotide-

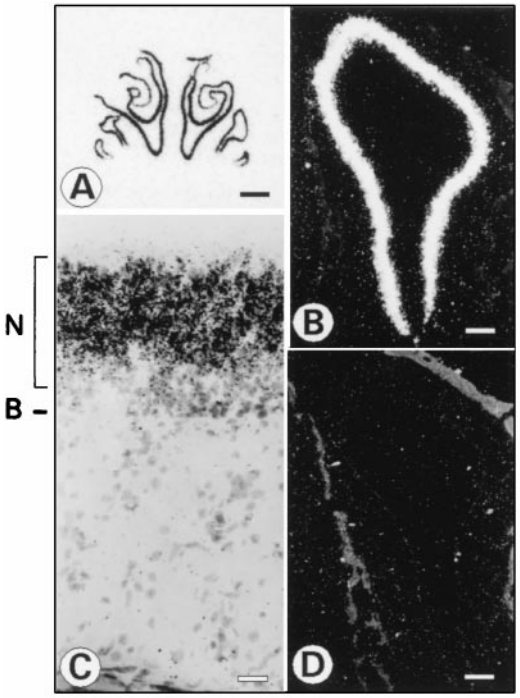

FIG. 4. Expression of CNG4.3 in rat olfactory epithelium. (*A*) Coronal section through the rat nasal cavity hybridized with a ^{35}S-labeled antisense RNA probe specific for CNG4.3. The nasal septum is in the center with the two nasal cavities on either side. Hybridization is seen throughout the entire extent of the olfactory epithelium. Autoradiographic exposure was for 6 days. The scale bar at bottom right equals 1 mm. (*B* and *D*) Darkfield photographs of consecutive sections hybridized to CNG4.3 specific antisense (*B*) or sense probe (*D*). Labeling of the olfactory epithelium only is seen with the antisense probe (*B*). The scalebar in (*B* and *D*) equals 140 μm. (*C*) High magnification brightfield photograph of a slide hybridized to the CNG4.3 specific antisense probe. A uniform signal of black silver grains is observed within the neuronal layer (N) of the olfactory epithelium. B, basal membrane. The scale bar equals 30 μm.

gated conductance with a K_a value for cAMP of 84 μM 12M (n = 9) (Fig. 5*A* and Table 1). The coexpression of CNG4.3 resulted in an approximately fivefold increase in cAMP affinity (K_a = 18.3 μM; n = 13). In cells cotransfected with CNG2 and CNG4.3 plasmids at a ratio of 1:4, the average K_a for cAMP was not significantly different from that found for equimolar coexpression of both subunits (not shown). Whereas CNG4.3 increased the cAMP affinity, it did not change significantly ($P > 0.05$) the cGMP affinity ($K_{a(CNG2)}$ = 1.6 μM, n = 22; $K_{a(CNG2/CNG4.3)}$ = 2.2 μM, n = 9; Fig. 5*B* and Table 1). CNG5 influenced the ligand affinities qualitatively similar as CNG4.3. It had no major effect on the cGMP affinity, but it significantly increased the affinity for cAMP (Fig. 5*A* and Table 1). Interestingly, patches of cells cotransfected with equimolar amounts of CNG2, CNG4.3, and CNG5 revealed a cyclic nucleotide-gated current that had a slightly higher affinity for cAMP (K_a = 5.5 μM, n = 17) than either the combination of CNG2 with CNG5 (K_a = 11 μM) or of CNG2 with CNG4.3 (K_a = 18 μM), respectively. Although the increase of cAMP affinity observed upon coexpression of all three subunits was only moderate, it was statistically significant ($P < 0.05$). Similar to the coexpression of CNG2 with one type of β subunit, the coexpression of both CNG4.3 and CNG5 subunits had no significant effect on cGMP affinity and Hill coefficients for channel activation (Table 1).

Beside its effect on cAMP affinity, the CNG4.3 subunit enhanced sensitivity to L-*cis* diltiazem (Fig. 5 *C* and *D*). At +60 mV, 100 μM L-*cis* diltiazem blocked ≈75% of the CNG2/CNG4.3 current whereas it only blocked 10% of the current

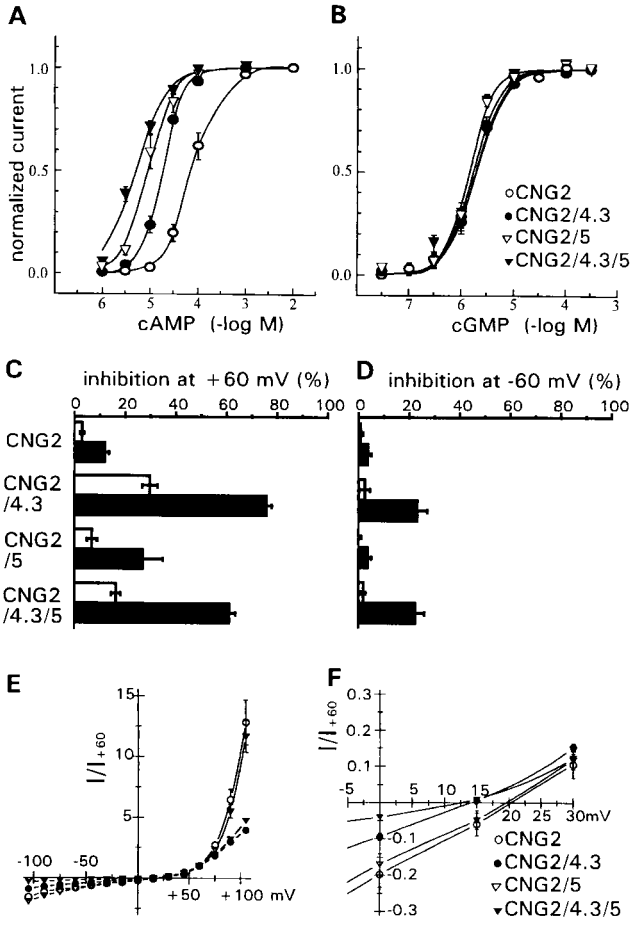

FIG. 5. Functional expression of rat olfactory CNG channel subunits in HEK293 cells. (*A* and *B*) cAMP (*A*) and cGMP (*B*) dose-response curves for currents induced by the expression of CNG2 (open circles), CNG2/CNG4.3 (closed circles), CNG2/CNG5 (open triangles), and CNG2/CNG4.3/CNG5 (filled triangles). Recordings were obtained from inside-out patches excised from HEK293 cells transfected with CNG channel expression plasmids. Curves were normalized to the response at saturating concentrations of cAMP or cGMP. Each point represents the mean ± SEM from 9 to 22 patches from at least two independent transfections. The solid lines are best fits calculated by the Hill equation (see *Materials and Methods*). (*C* and *D*) Inhibition of CNG channel currents by 10 μM (white boxes) and 100 μM (black boxes) L-*cis* diltiazem at a membrane potential of +60 mV (*C*) and −60 mV (*D*). Currents were activated by a saturating cGMP concentration (300 μM). The individual bars represent the mean ± SEM from 6 to 13 patches. (*E*) Current-voltage relations of CNG channels in the presence of 10 mM extracellular Ca^{2+} (for symbols see *F*). All of the currents were activated by 300 μM cGMP and normalized to the current at +60 mV. The points represent means ± SEM from 6 to 8 patches. (*F*) Enlargement of the current-voltage relations shown in *E* displaying the voltage range from −5 mV to +30 mV.

induced by CNG2 alone. CNG5 also had some influence on the block by L-*cis* diltiazem; however, its effect significantly was less pronounced than that observed with CNG4.3 (30% vs. 75% block at +60 mV with CNG5 and CNG4.3, respectively). The current measured in the presence of all three subunits revealed a sensitivity to L-*cis* diltiazem similar to that of the CNG2/CNG4.3 channel (≈60% block at +60 mV by 100 μM diltiazem). This sensitivity is in the range of that of native olfactory CNG channels (K_i of 70 μM at +100 mV; ref. 17). As observed in native channels, the L-*cis* diltiazem block was voltage-dependent being stronger at positive than at negative voltages (Fig. 5 *C* and *D*).

We next investigated the influence of CNG4.3 on the interaction of the CNG channel with Ca^{2+}. Coexpression of

Table 1. Apparent K_a values, Hill coefficients (v), and relative Ca^{2+} permeabilities ($P_{Ca^{2+}}/P_{Na^+}$) of homomeric and heteromeric olfactory CNG channels

	cAMP			cGMP			10 mM $[Ca^{2+}]_o$		
channels	*n*	K_a, μM	v	*n*	K_a, μM	v	*n*	V_{rev}, mV	$P_{Ca^{2+}}/P_{Na^+}$
CNG2	9	84.0 ± 13.7	1.86 ± 0.23	22	1.55 ± 0.16	2.27 ± 0.19	6	+21.0 ± 2.85	15.5
CNG2/4.3	13	18.3 ± 1.14	2.29 ± 0.32	9	2.18 ± 0.38	1.67 ± 0.12	8	+13.9 ± 0.48	7.3
CNG2/5	11	11.3 ± 2.83	2.37 ± 0.30	8	1.94 ± 0.19	1.76 ± 0.15	7	+19.4 ± 2.71	13.2
CNG2/4.3/5	17	5.46 ± 0.67	1.55 ± 0.12	18	1.36 ± 0.10	1.87 ± 0.19	6	+12.8 ± 0.56	6.4

n, number of patches. V_{rev} reversal potential. Results are given as mean ± SEM. K_a values and Hill coefficients were determined at a membrane potential of +60 mV.

CNG4.3 weakened the outward rectification of the current in the presence of 10 mM extracellular Ca^{2+} (Fig. 5*E*). CNG4.3 also reduced the amplitude of the inward current at hyperpolarizing membrane potentials and shifted the reversal potential of the current for ≈7 mV to more negative potentials with respect to the reversal potential of CNG2 measured under the same conditions (Fig. 5*F* and Table 1). The resulting theoretical permeability ratio $P_{Ca^{2+}}/P_{Na^+}$ according to ref. 23 was 7.3 for the CNG2/CNG4.3 channel and 15.5 for the CNG2 channel. CNG5 had little influence on interaction with Ca^{2+}. The reversal potential of the CNG2/CNG5 channel did not differ significantly ($P > 0.05$) from that of the homomeric CNG2 channel. The reversal potential observed when all three subunits were coexpressed was similar to that of the CNG2/CNG4.3 current (Fig. 5*F* and Table 1).

DISCUSSION

We have cloned an isoform (CNG4.3) of the rod photoreceptor β subunit from rat olfactory epithelium. CNG4.3 shares the transmembrane domain, the cyclic nucleotide binding site, and the C terminus with the previously cloned photoreceptor β subunit (20) but contains a much shorter N terminus. In particular, the glutamic-acid rich domain that is present in photoreceptor CNG4 is completely missing in CNG4.3. We found no evidence for the expression of a cytoplasmic glutamic acid-rich protein in olfactory epithelium. From the intron/exon organization determined, we suggest that the generation of the CNG4.3 transcript most likely occurs via use of an internal promoter present in the intron upstream of exon β2a. Recently, a similar mechanism has been postulated to explain the transcription of a "short" photoreceptor CNG4 isoform in human retina (12, 14). However, in this case, transcription is initiated at a position localized downstream from the CNG4.3 starting point. Other short CNG4 isoforms have been identified from bovine testis (22). Thus, the heterogeneity of CNG4 transcripts in different species and tissues may result from the use of various internal promotors present within the CNG4 gene and from alternative splicing of the primary transcripts.

CNG4.3 is expressed specifically in olfactory neurons whereas transcripts were not detectable in the supporting and basal cell layers of the olfactory epithelium. A similar expression pattern was described (10, 11) for the CNG2 subunit and the CNG5 subunit being in line with our own results. By contrast, rod (CNG1) and cone (CNG3) photoreceptor α subunits were not detected in the olfactory system. Taken together, these data indicate that CNG2, CNG4.3, and CNG5 subunits coexist in olfactory neurons.

Like other CNG4 isoforms, CNG4.3 does not form a functional CNG channel by itself. However, it assembles with CNG2 to produce a heteromeric channel with properties different from those of the homomeric CNG2 channel. The most prominent effect introduced by CNG4.3 is the increase of cAMP sensitivity. By contrast, CNG4.3 has no effect on the affinity for cGMP when coexpressed with CNG2. The K_a ratio for cAMP vs. cGMP is eight for the heteromeric CNG2/CNG4.3 channel. This value matches much better the K_a ratio determined for the wild-type olfactory channel (K_a ratio of ≈2.5, ref. 17) than the ratio of the homomeric CNG2 channel (K_a ratio of 64) does. Coexpression of CNG2, CNG4.3, and CNG5 results in a two- to threefold increase of cAMP affinity with respect to the CNG2/CNG4.3 and CNG2/CNG5 currents. The resulting K_a ratio of the triple combination is approximately four. This value is almost equal to that observed for the wild-type channel, suggesting that a CNG channel containing three different subunits may exist *in vivo*. However, because the current measured when all three of the subunits are coexpressed is distinguished only from the CNG2/CNG4.3 current by the moderate increase of cAMP affinity it cannot be decided conclusively at the moment whether or not CNG5 is assembled into the heteromeric channel in the presence of CNG4.3.

CNG4.3 has a profound effect on the channel properties in the presence of extracellular Ca^{2+}. First, CNG4.3 weakens the outward rectification of the current when coexpressed with the α subunit. This finding is consistent with the recent observation that the rod photoreceptor CNG4 isoform exerts a similar effect when coexpressed with the rod α subunit (12). Secondly, CNG4.3 reduces the relative permeability of the channel for Ca^{2+}. Nevertheless, the heteromeric CNG2/CNG4.3 channel still reveals an approximately sevenfold higher permeability for Ca^{2+} than for Na^+. The permeability ratio measured in the presence of CNG4.3 is in the range of the ratio calculated for the native olfactory channel (ratio of 6.5, ref. 26) suggesting that CNG4.3 forms a subunit of this channel. Unlike the CNG4.3 subunit, CNG5 has no major influence on both current rectification and calcium permeability when coexpressed with CNG2. This finding is in line with a recent study (27) showing that the exchange of the glutamate residue representing the binding site for extracellular Ca^{2+} in the pore of CNG channel α subunits by an aspartate residue which is found at the equivalent position in CNG5 had no major effect on the blockade by extracellular Ca^{2+}.

In summary, our data indicate that CNG4.3 is an essential subunit of the native olfactory CNG channel. Given the good correlation between the functional properties of the CNG2/CNG4.3 channel with those of the native olfactory channel (1, 4, 17, 28), it is likely that the CNG2/CNG4.3 channel also is expressed *in vivo*. The role of the CNG5 subunit should be reconsidered based on our experiments. CNG5 may form a heteromeric channel with CNG2 as has been suggested (10, 11) but may also assemble with both CNG2 and CNG4.3 to create a distinct olfactory CNG channel. In addition, the CNG5 subunit may form an NO-activated homomeric channel in a subset of olfactory neurons (18). The possible coexistence of different CNG channel types could explain the heterogeneity of CNG channels observed in individual olfactory neurons (28, 29). The variation of β subunit expression could be the molecular basis for this variability. Finally, the finding, that distinct CNG4 isoforms assemble with both photoreceptor (13, 22) and olfactory α subunits to form functional CNG channels suggests that the CNG4 subunit may fulfill a general role for normal CNG channel function in different sensory transduction pathways.

We thank H. Breer and J. Strotmann for providing the sections of rat olfactory epithelium. L-*cis* diltiazem was kindly provided by H. Yabana (Tanabe Seiyaku Co., Ltd.). This work was supported by grants from Deutsche Forschungsgemeinschaft, Bundesministerium für Bildung und Forschung, and Fond der Chemie.

1. Zufall, F., Firestein, S. & Shepherd, G. M. (1994) *Annu. Rev. Neurosci.* **23,** 577–607.
2. Breer, H., Raming, K. & Krieger, J. (1994) *Biochem. Biophys. Acta* **1224,** 277–287.
3. Lowe, G. & Gold, G. H. (1993) *Nature (London)* **366,** 283–286.
4. Finn, J. T, Grunwald, M. E. & Yau, K. W. (1996) *Annu. Rev. Neurosci.* **58,** 395–426.
5. Biel, M., Zong, X. & Hofmann, F. (1996) *Trends Cardiovasc. Med.* **6,** 274–280.
6. Dhallan, R. S., Yau, K. W., Schrader, K. A. & Reed, R. R. (1990) *Nature (London)* **347,** 184–187.
7. Kaupp, U. B., Niidome, T., Tanabe, T., Terada, S., Bönigk, W., Stühmer, W., Cook, N. J., Kangawa, K., Matsuo, H., Hirose, T., *et al.* (1989) *Nature (London)* **342,** 762–766.
8. Weyand, I., Godde, M., Frings, S., Weiner, J., Müller, F., Altenhofen, W., Hatt, H. & Kaupp, U. B. (1994) *Nature (London)* **368,** 859–863.
9. Biel, M., Zong, X., Distler, M., Bosse, E., Klugbauer, N., Murakami, M., Flockerzi, V. & Hofmann, F. (1994) *Proc. Natl. Acad. Sci. USA* **91,** 3505–3509.
10. Liman, E. R. & Buck L. B. (1994) *Neuron* **13,** 611–621.
11. Bradley, J., Li, J., Davidson, N., Lester, H. A. & Zinn, K. (1994) *Proc. Natl. Acad. Sci. USA* **91,** 8890–8894.
12. Chen, T. Y., Peng, Y. W., Dhallan, R. S., Ahamed, B., Reed, R. R. & Yau, K. W. (1993) *Nature (London)* **362,** 764–767.
13. Körschen, H. G., Illing, M., Seifert, R., Sesti, F., Williams, A., Gotzes, S., Colville, C., Müller, F., Dose, A., Godde, M., *et al.* (1995) *Neuron* **15,** 627–636.
14. Ardell, M. D., Aragon, I., Oliveira, L., Porche, G. E., Burke, E. & Pittler, S. J. (1996) *FEBS Lett.* **389,** 213–218.
15. Colville, C. A. & Molday, R. S. (1996) *J. Biol. Chem.* **271,** 32968–32974.
16. Brunet, L. J., Gold, G. H & Ngai, J. (1996) *Neuron* **17,** 681–693.
17. Frings, S., Lynch, J. W. & Lindemann, B. (1992) *J. Gen. Physiol.* **100,** 45–67.
18. Broillet, M. C. & Firestein, S. (1997) *Neuron* **18,** 951–958.
19. Berghard, A., Buck, L. B. & Liman, E. R. (1996) *Proc. Natl. Acad. Sci. USA* **93,** 2365–2369.
20. Sautter, A., Biel, M. & Hofmann, F. (1997) *Mol. Brain Res.* **47,** 171–175.
21. Ludwig, A., Flockerzi, V. & Hofmann, F. (1997) *J. Neurosci.* **17,** 1339–1349.
22. Biel, M., Zong, X., Ludwig, A., Sautter, A. & Hofmann, F. (1996) *J. Biol. Chem.* **271,** 6349–6355.
23. Lewis, C. A. (1979) *J. Physiol.* **286,** 417–445.
24. Sugimoto, Y., Yatsunami, K., Tsujimoto, M., Khorana, H. G. & Ichikawa, A. (1991) *Proc. Natl. Acad. Sci. USA* **88,** 3116–3119.
25. Ardell, M. D., Makhija, A. K., Oliveira, L., Miniou, P., Viegas-Péquignot, E. & Pittler, S. J. (1996) *Genomics* **28,** 32–38.
26. Kurahashi, T. & Shibuya, T. (1990) *Brain Res.* **515,** 261–268.
27. Root, M. J. & MacKinnon, R. M. (1993) *Neuron* **11,** 459–466.
28. Nakamura, T. & Gold G. H. (1987) *Nature (London)* **325,** 442–444.
29. Thüraüf, N., Gjuric, M. & Hatt, H. (1996) *Eur. J. Neurosci.* **8,** 2080–2089.
30. Breathnach, R. & Chambon, P. (1981) *Annu. Rev. Biochem.* **50,** 349–383.